Bulletin of the JSME Vol.3, No.6, 2016
Mechanical Engineering Journal

Feasibility study on characterization of non-Gaussian rough surface by ultrasonic reflection method with the Kirchhoff theory

Muhammad Nur Farhan SANIMAN* and Ikuo IHARA**
*Graduate School of Engineering, Nagaoka University of Technology
1603-1 Kamitomioka, Nagaoka, Niigata 940-2137, Japan
E-mail: moll@stn.nagaokaut.ac.jp
**Department of Mechanical Engineering, Nagaoka University of Technology
1603-1 Kamitomioka, Nagaoka, Niigata 940-2137, Japan

Received 3 March 2016

Abstract
The fundamental study on the ultrasonic characterization of non-Gaussian rough surface of a material is carried out. In this study, a theoretical relationship among ultrasonic reflection coefficient at normal incidence, root mean square roughness *Rq*, and skewness *Rsk* (which is the measure of symmetrical level of a height distribution) has been derived. In the derivation, a Gaussian curve fitting to the non-Gaussian height distribution of a rough surface is effectively performed so that the Kirchhoff theory of wave scattering from a rough surface can be utilized. In order to verify the validity of the derived relationship, air-coupled ultrasonic pulse-echo measurements with normal incident configuration at center frequency of 0.35 MHz have been conducted to a series of sandpapers having various *Rq* and *Rsk* values. From the measured ultrasonic reflection coefficient of each sandpaper, the *Rq* values of the sandpapers have been estimated from the derived relationship with known values of skewness of the sandpapers and then compared to those measured by a mechanical stylus profiler. It is found that the *Rq* values estimated by the ultrasonic method and the stylus profiler almost agree with each other. Thus, the validity of the derived theoretical relationship is demonstrated.

Key words : Air-coupled ultrasound, Roughness, Skewness, Non-Gaussian surfaces, Johnson distribution

1. Introduction

The characterization of topographic roughness of material surfaces is important because it is directly related to the tribological properties and the contact mechanic of the rough surfaces (Kubiak, et. al., 2011, Uehara and Sakurai, 2002). Commonly, such roughness properties of the material surfaces are evaluated at post processing (Miko and Nowakowski, 2012, Asiltürk and Akkuş, 2011). However, a late detection of surface defects or poor surface qualities could lead to an increase in the production's cost and time. Thus, on-line or *in-situ* measurements are particularly important in order to control the machining process in real time. Although the so-called stylus profilometry is well known and widely employed to characterize the surface roughness, such method is not always acceptable for some practical uses because it is a contact method and therefore, difficult to be applied in the on-line measurements. In order to overcome such drawbacks, alternative noncontact methods with faster response are needed.

Recently, ultrasonic method has been proposed as one of the alternative methods to characterize the roughness of material surfaces (Saniman and Ihara, 2014, Ramesh, et al., 2013, Suryono, et al., 2010, Mitri, et al., 2009, Forouzbakhsh, et al., 2009, Sukmana and Ihara, 2007, Gunarathne and Christidis, 2001, Blessing, et al., 1993, Billy, et al., 1980). In fact, such method is very promising especially for the characterization of very rough surfaces up to 1000 μm where the optical method cannot be applied due to the short wavelength of light (Forouzbakhsh, et al., 2009, Blessing, et al., 1993). To date, many experimental attempts have been conducted to ultrasonically characterize the

Paper No.16-00162
J-STAGE Advance Publication date: 12 July, 2016
[DOI: 10.1299/mej.16-00162]

roughness of the material surfaces either by water immersion or air-coupling technique (Saniman and Ihara, 2014, Blessing, et al., 1993, Gunarathne and Christidis, 2001, Sukmana and Ihara, 2007). In such ultrasonic method, the surface roughness has been estimated from the measured reflection coefficient of ultrasonic waves using the Kirchhoff theory of wave scattering (Ogilvy, 1991). Due to the mathematics involved, the material surfaces to be evaluated are assumed to have a Gaussian or symmetrical height distribution. However, material surfaces polished mechanically or treated chemically often have an asymmetrical or skewed height distribution. In fact, some of the material surfaces are deliberately fabricated or designed to have a skewed or non-Gaussian height distribution, such as the surface of a piston (Jeng, 1996), asphalt road (Wen, 1997), and water channel (Taylor, et al., 2006). Furthermore, it has been reported that the topographic roughness of material surfaces might change from a Gaussian distribution to the non-Gaussian one especially when the material surfaces are subjected to processes such as wear and friction (Srivastava, et al., 2007, Yuan, et al., 2008, Eriten, et al., 2011). Thus, a new approach that considers the effect of non-Gaussian properties to the reflection coefficient is needed in order to ultrasonically characterize such non-Gaussian surfaces.

In this study, an attempt to characterize the roughness of the non-Gaussian rough surfaces has been conducted where a theoretical relationship among ultrasonic reflection coefficient at normal incidence, root mean square (r.m.s.) roughness *Rq*, and skewness *Rsk* has been developed. Such relationship has been derived based on a proposed method of optimally fitting a Gaussian curve to the non-Gaussian height distribution (the Johnson distribution). Then, in order to verify the validity of the proposed curve fitting method as well as the derived theoretical relationship, experimental verifications have been conducted where a series of sandpapers having various values of *Rq* and *Rsk* are insonified with a 0.35 MHz air-coupled ultrasound at normal incidence. The *Rq* of the specimens are then estimated from the measured ultrasonic reflection coefficient and compared to those measured by a stylus profiler. The agreement between both ultrasonic and profilometric *Rq* values, which indicates the validity of the derived relationship, will be discussed.

2. The properties of non-Gaussian surfaces

2.1 Statistical parameters of the height probability density function (PDF)

The properties of surface profiles can be described statistically by its probability density function (PDF) of height *p(h)*, which is the frequency distribution of points on a surface profile with height equal to *h*. The shape of the height PDF could provide useful information about the nature of the surface profiles that can be expressed mathematically by four statistical parameters, which are the mean *h**, standard deviation or r.m.s. roughness *Rq*, skewness *Rsk*, and kurtosis *Rku*, that are given by (Gadelmawla, 2002)

$$h^* = \sum_{i=0}^{N} \frac{p(h_i)h_i}{N}, \tag{1}$$

$$Rq = \sqrt{\frac{1}{N}\sum_{i=1}^{N}(h_i - h^*)^2 p(h_i)}, \tag{2}$$

$$Rsk = \frac{1}{NRq^3}\sum_{i=1}^{N}(h_i - h^*)^3 p(h_i), \tag{3}$$

$$Rku = \frac{1}{NRq^4}\sum_{i=1}^{N}(h_i - h^*)^4 p(h_i), \tag{4}$$

respectively, where *N* is the samples number.

Skewness *Rsk* is a measure of symmetrical level of a height PDF and sensitives to occasional deep valleys or high peaks where the existences of such surface features could change the height PDF of a surface profile from a Gaussian distribution to the non-Gaussian one. Thus, depending on the symmetrical level of the height PDF, the value of *Rsk* may vary as shown in Fig. 1. Zero skewness (*Rsk* = 0) represents a symmetrical height PDF of a surface profile with as many peaks and valleys. Positive skewness (*Rsk* > 0) represents an asymmetrical height PDF of a surface profile with high peaks or filled valleys, while negative skewness (*Rsk* < 0) represents those with deep scratches or removed peaks. On the other hand, kurtosis *Rku* is the measure of 'peakedness' or spikiness of a height PDF as shown in Fig. 2. A Gaussian distribution has kurtosis equal to 3 (*Rku* = 3). A platykurtic height PDF (*Rku* < 3) corresponds to a flatter

[DOI: 10.1299/mej.16-00162]

distribution which represents a gently undulating surface profile while a leptokurtic height PDF (*Rku* > 3) is the opposite.

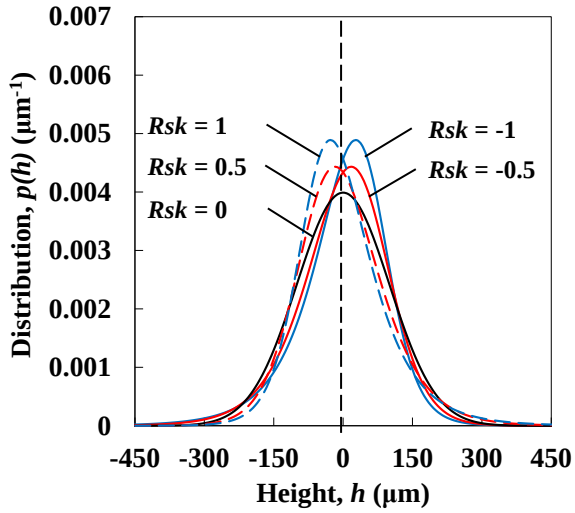

Fig. 1 Height distribution for various skewness *Rsk* values (*h** = 0, *Rq* = 100 µm, and *Rku* is given by Eq. (17)).

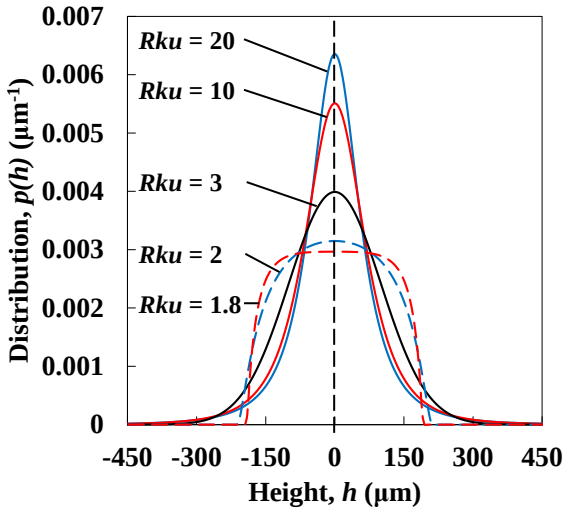

Fig. 2 Height distribution for various kurtosis *Rku* values (*h** = 0, *Rq* = 100 µm, and *Rsk* = 0).

2.2 Gaussian and Johnson height distribution

Gaussian distribution $p(h)_G$ is a very well-known and commonly used distribution to describe the height PDF of material surfaces and is given by

$$p(h)_G = \frac{1}{Rq\sqrt{2\pi}} \exp\left(-\frac{\{h-h^*\}^2}{2Rq^2} \right). \tag{5}$$

From Eq. (5), the statistical properties of the Gaussian distribution are determined by only two parameters, which are *h** and *Rq*. This means that there is no information about *Rsk* can be extracted from Eq. (5), yet it is known that *Rsk* is equal to zero due to the fact that a Gaussian distribution is always symmetry. Therefore, Johnson distribution (Johnson, 1949) is introduced in this study in order to study the effect of *Rsk* to the shape of the height PDF as well as to characterize the non-Gaussian rough surfaces. Such things are possible because the Johnson distribution has four statistical parameters which make it very flexible in describing any kind of unimodal non-Gaussian height PDF. In fact, the similar approach has been applied in many studies related to the skewness effect onto the tribological properties of the non-Gaussian rough surfaces (Wang, et. al., 2015, Yan, et. al., 2014). The unbounded type of the Johnson distribution $p(h)_J$ is given by

$$p(h)_J = \frac{\delta}{\sqrt{2\pi\left(x^2+1\right)}} \exp\left\{ -\frac{\gamma + \delta \cdot \ln\left(x + \sqrt{x^2+1} \right)^2}{2} \right\}, \tag{6}$$

where

$$x = (h-\xi)/\lambda. \tag{7}$$

Here, γ, δ, λ, and ξ are the parameters that determine the shape of the Johnson distribution. Such parameters can be estimated from the values of *h**, *Rq*, *Rsk*, and *Rku* by using an iterative numerical algorithm proposed by Tuenter (Tuenter, 2001), which can be simplified as follow:

1. Define the values of *h**, *Rq*, *Rsk*, and *Rku*.
2. Perform Newton-Raphson iterations to calculate *w* which is the value that satisfies *f(w)* = *Rsk*, where *f(w)* is given by

[DOI: 10.1299/mej.16-00162]

$$f(w) = \left(w - 1 - m\right)\left(w + 2 + \frac{1}{2}m\right)^2 = Rsk. \tag{8}$$

3. Calculate γ, δ, λ, and ξ by using the following equations, respectively,

$$\gamma = \frac{-\mathrm{sgn}(Rsk)}{\sqrt{\ln w}} \sinh^{-1}\sqrt{\frac{w+1}{2w}\left(\frac{w-1}{m} - 1\right)}, \tag{9}$$

$$\delta = \frac{1}{\sqrt{\ln w}}, \tag{10}$$

$$\lambda = \frac{Rq}{w-1}\sqrt{\frac{2m}{w+1}}, \tag{11}$$

$$\xi = h^* - \mathrm{sgn}(Rsk)\frac{Rq}{w-1}\sqrt{w-1-m}, \tag{12}$$

where

$$m = -2 + \sqrt{4 + 2\left[w^2 - \frac{Rku + 3}{w^2 + 2w + 3}\right]}. \tag{13}$$

The function sgn(*Rsk*) is -1 for *Rsk* < 0, 0 for *Rsk* = 0, and +1 for *Rsk* > 0. The height PDFs having various *Rsk* and *Rku* values are shown in Fig. 1 and Fig. 2, respectively, where such height PDFs have been calculated based on the Johnson distribution given by Eq. (6). It can be observed how the values of *Rsk* and *Rku* are influencing the shape of the height PDFs. Note that in Fig. 1, the values of *Rku* are not constant and given by Eq. (17) in Section 4, while in Fig. 2, *Rsk* is equal to zero for all *Rku* values. The values of h^* and *Rq* are 0 and 100 μm, respectively, for both figures.

3. Descriptions of the optimum curve fitting method of Gaussian to Johnson distribution

Figure 3 shows the examples of arbitrary skewed rough surface profiles with *Rsk* = 0.0, 1.0, and -1.0 and its corresponding height PDFs which are well approximated by the Johnson curve (denotes by the red dashed line). It can be observed that when the *Rsk* increases positively, the surface profile tends to has more high peaks, and inversely, when the *Rsk* increases negatively, the surface profile tends to has more deep valleys. Generally, such high peaks or deep valleys can be represented by the tail of the height PDFs. Moreover, such high peaks or deep valleys also not only are having large height deviation *dh* values from the mean height, but also are having large gradient *dh/dx* values compared to the other parts of the surface profile. Thus, when such surface features are insonified with ultrasonic waves at normal incidence (θ_{inc} = 0°), the reflected ultrasonic waves will be scattered incoherently into non-specular directions due to the large phase difference $\Delta\varphi$, which is given by (Ogilvy, 1987)

$$\Delta\phi = k\left\{dh(\cos\theta_{inc} + \cos\theta_{ref}) + dx(\sin\theta_{inc} - \sin\theta_{ref})\right\}. \tag{14}$$

Here, *k* is the wavenumber, θ_{inc} and θ_{ref} are the incidence and reflection angle, respectively. In contrast, the ultrasonic waves will be coherently reflected into the specular directions when the non-high peaks or non-deep valleys surface areas with small *dh* and *dh/dx* values (which are called as the plateau or bearing surface areas) are insonified with ultrasonic waves. Thus, it is assumed that such bearing surface areas not only are dominant in determining the intensity of the coherent component of reflected ultrasonic waves at normal incidence, but also have a Gaussian height PDF $p(h)'_G$ with standard deviation or r.m.s. roughness *Rq'*.

In order to determine such *Rq'* of a non-Gaussian rough surface with known values of *Rq* and *Rsk*, an optimum method of fitting a half-Gaussian curve to the non-tail side of the Johnson distribution $p(h)_J$ is proposed, which is given by the following steps:

[DOI: 10.1299/mej.16-00162]

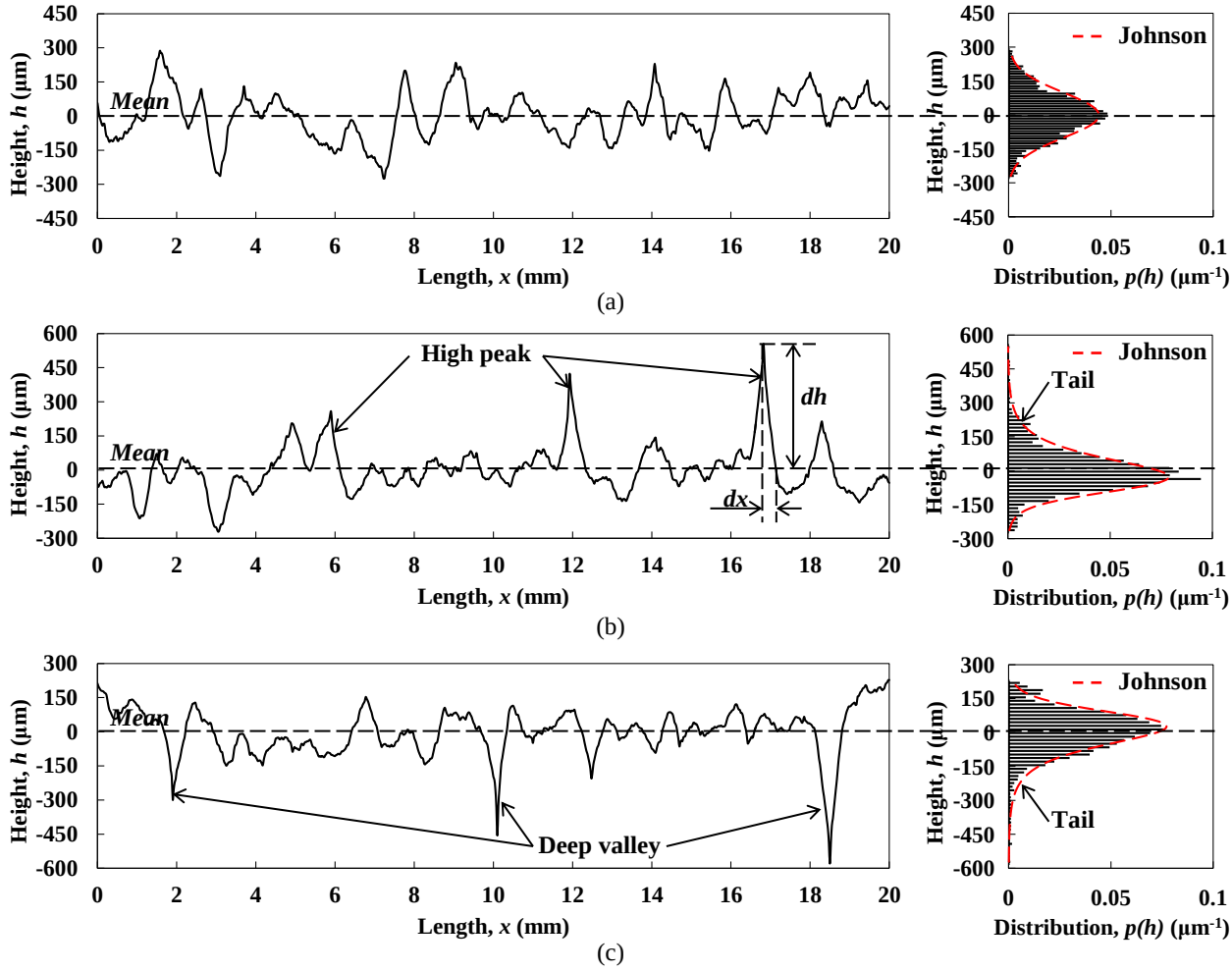

Fig. 3 Non-Gaussian random rough surfaces and its corresponding height PDFs having *Rsk* equal to (a) 0.0, (b) +1.0, and (c) -1.0 with constant values of $h^* = 0$ μm and $Rq = 100$ μm.

1. Define the values of *Rq*, *Rsk*, and *Rku* while h^* is kept constant at 0.
2. Determine the values of γ, δ, λ, and ξ by using the Tuenter algorithm mentioned in section 2.2.
3. Calculate the Johnson distribution $p(h)_J$ using Eq. (6) for an appropriate range of h. Such h in the range of $\pm 6Rq$ with an interval of $0.01Rq$ is found to be sufficient.
4. Let t as the mode value of $p(h)_J$ (t is the value of h when $p(h)_J$ is at the maximum value). Note that t is also the value that marks the boundary between the tail and non-tail side of $p(h)_J$.
5. Calculate Rq' of the non-tail side of $p(h)_J$, which is given by

$$Rq' = \sqrt{2\sum_{i=1}^{M}\left\{-\mathrm{sgn}(Rsk)h_i - t\right\}^2 p(h_i)_J}\,. \tag{15}$$

   Here, M is the count of h of the non-tail side of $p(h)_J$.
6. Calculate the corresponding Gaussian distribution curve $p(h)'_G$ that has the same range of h in step 3 using the calculated values of t and Rq' from steps 4 and 5, respectively, for fitting the non-tail side of the calculated $p(h)_J$. Such $p(h)'_G$ is given by

$$p(h)'_G = \frac{1}{Rq'\sqrt{2\pi}}\exp\left(-\frac{\left\{h-t\right\}^2}{2Rq'^2}\right). \tag{16}$$

7. Determine the correlation coefficient R^2 between the $p(h)'_G$ and $p(h)_J$ of the non-tail side of the distributions.

[DOI: 10.1299/mej.16-00162]

8. Change the value of *Rku* in step 1 and repeat steps 2 to 7 until the maximum value of R^2 is found. The values of *Rq'* and *Rku* when R^2 is at the maximum value are taken as the optimum values.

The proposed method is designed to determine the optimum *Rku* and the corresponding *Rq'* that give the best fitting result between the Gaussian and Johnson distribution for the given values of *Rq* and *Rsk*. Additionally, the fitting process should be repeated for various *Rq* and *Rsk* in order to study the relationship among *Rq'*, *Rq*, *Rsk*, and *Rku*. The obtained parameters are expected to be used in formulating the theoretical relationship among reflection coefficient, *Rq* and *Rsk* of the non-Gaussian surface profiles.

4. Derivation of the theoretical relationship among reflection coefficient, *Rq*, and *Rsk*

In this study, the numerical calculations based on the proposed curve fitting method have been conducted for *Rq* and *Rsk* in the range of 0.001 to 1000 μm and -1.2 to 1.2, respectively. In fact, such ranges can be considered as the practical range of engineering surfaces (Whitehouse, 2003). Figure 4 shows the examples of such fitting processes for artificial height PDFs having *Rsk* = 0.0, -0.5, and -1.0 with constant values of *h** = 0 and *Rq* = 100 μm. It can be observed that when the negative *Rsk* increases, not only the value of *Rq'* decreases, but also the value of *t* is biased to the positive side of *h**, which indicates that a large region of such surface bearing areas is concentrated slightly above the surface mean height as shown in Fig. 3(c).

Furthermore, from the best fitting results, it is found that regardless of *Rq*, the optimum values of *Rku* is depending on the value of *Rsk*, which can be approximated by

$$Rku = 1.89Rsk^2 + 1.65Rsk + 3. \tag{17}$$

The fact that *Rku* became a function of *Rsk* means that the non-tail side of the Johnson distribution can only be fitted by a Gaussian distribution at the specific combinations of *Rsk* and *Rku* given by Eq. (17). Such increment of *Rku* with *Rsk* can be considered as the common properties of engineering surfaces, especially those that have been produced by machining processes such as honing and milling (Whitehouse, 2003). Moreover, from the calculated *Rq'* for each combination of *Rq* and *Rsk*, the relationship among *Rq'*, *Rq*, and *Rsk* have been approximated from the interpolation of the ratio of *Rq'* to *Rq* with *Rsk* as shown in Fig. 5 and is given by

$$Rq' = \frac{1.864 + 0.059|Rsk|}{1.864 + |Rsk|} Rq. \tag{18}$$

Note that the absolute value of skewness, |*Rsk*|, is used in Eq. (18) because the identical trends are observed for both positive and negative *Rsk*. In addition, Fig. 5 indicates that for a constant value of *Rq*, when |*Rsk*| increases, *Rq'* decreases. This finding suggests that for largely skewed rough surfaces with deep valleys or high peaks, the surface's bearing areas are having small height variations and the degree of such variations are depending on the *Rsk* value of the surface profiles.

As mentioned before, *Rq* is the r.m.s. roughness of the whole surface areas having skewed height PDF while *Rq'* is the r.m.s. roughness of a large region of the surface bearing areas having Gaussian height PDF. Because of *Rq'* is

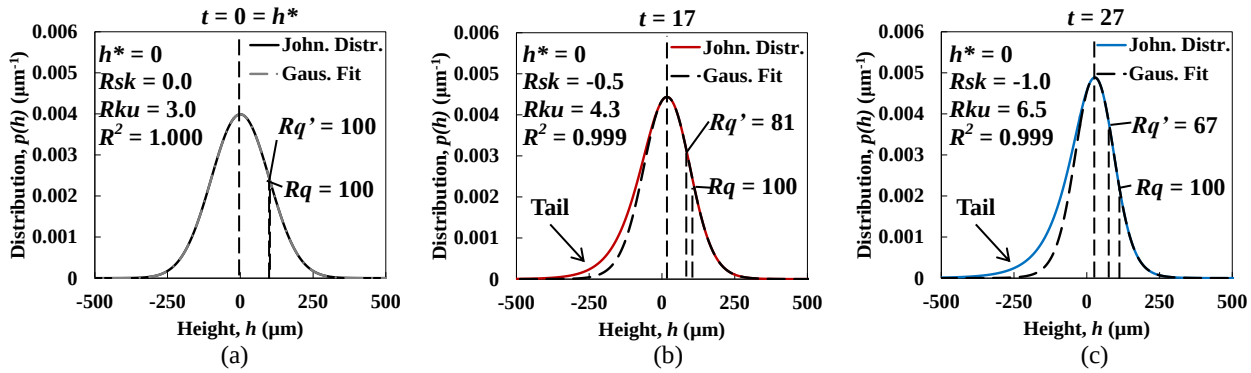

Fig. 4 Gaussian to Johnson curve fitting process for the height PDFs having *Rsk* equal to (a) 0.0, (b) -0.5, and (c) -1.0 with constant values of *h** = 0 μm and *Rq* = 100 μm.

[DOI: 10.1299/mej.16-00162]

dominant in determining the intensity of the coherent component of the reflected ultrasonic waves, we proposed that *Rq'* in Eq. (18) is substituted into the original Kirchhoff equation of reflection coefficient (Ogilvy, 1991), which is given by

$$I_{OK} = \frac{A_{coh}}{A_0} = \exp(-2k^2 Rq^2), \tag{19}$$

and the resulting equation is given by

$$I_{MK} = \exp(-2k^2 Rq'^2) = \exp\left(-2k^2 Rq^2 \left\{ \frac{1.864 + 0.059\,|Rsk|}{1.864 + |Rsk|} \right\}^2 \right), \tag{20}$$

which have been derived by following the similar mathematical works by Ogilvy (Ogilvy, 1991) and explained in Appendix A. Here, A_{coh} and A_0 are the reflected wave amplitude from a rough and a perfect smooth surface, respectively. Note that *I* is observed at a distance *r* away from the surface in the far field region. Equation (20), which is considered as the theoretical relationship among the reflection coefficient *I*, *Rq*, and *Rsk*, is proposed to be used to characterize the non-Gaussian rough surfaces. It is noted that such relationship is limited only to the reflection coefficient at normal configuration ($\theta_{inc} = \theta_{ref} = 0°$) of a random rough surface having a unimodal non-Gaussian height PDF.

Using Eq. (20), the theoretical changes of *I* with *Rq* that propagate in air at frequency 0.4 MHz for |*Rsk*| = 0.0, 0.5, and 1.0 are numerically calculated and shown in Fig. 6. It is found that there are distinctive changes of *I* with *Rq* for different *Rsk* values, which indicate that *I* significantly depends on *Rq* and *Rsk*. It is also found that for a constant value of *Rq*, when |*Rsk*| increases, *I* also increases. This is because *Rq'* decreases when *Rsk* increases, where a small *Rq'* value leads to a small phase difference in the reflected ultrasonic waves and thus, contribute to the generation of a high intensity coherent components. Such finding suggests that *Rq* can be estimated from Eq. (20) with known values of *I* and *Rsk*, or vice versa. Thus, it is demonstrated that the derived theoretical relationship based on the proposed curve fitting method could be useful in the quantitative characterization of non-Gaussian rough surfaces by the ultrasonic reflection method.

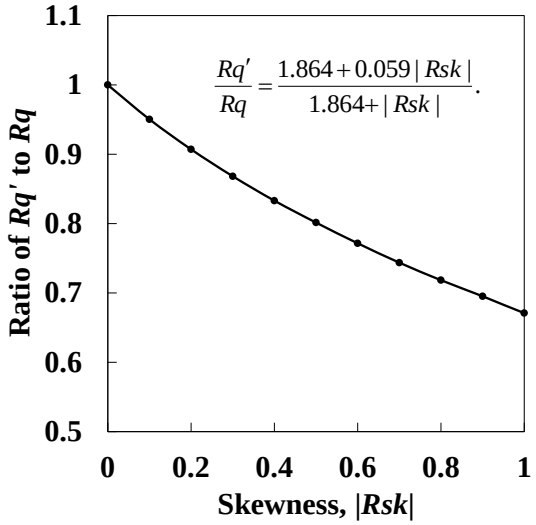

Fig. 5 Ratio of *Rq'* to *Rq* with *Rsk* estimated numerically by the proposed method of Gaussian to Johnson curve fitting.

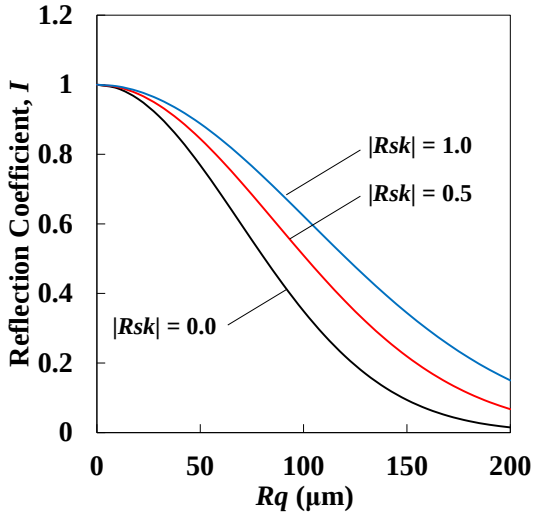

Fig. 6 Theoretical changes of the reflection coefficient with *Rq* for various *Rsk* of a 0.4 MHz ultrasonic wave in air.

5. Experimental validation

5.1 Experimental setup

Since it is important to verify the validity of the derive relationship given by Eq. (20), experimental validations consist of the roughness measurements using an air-coupled ultrasonic reflection method have been conducted. In the measurements, a series of sandpapers having various Rq_{SP} and Rsk_{SP} values, which have been measured by using a mechanical stylus profilometer (SP), is used as the specimens. Such specimens are bonded to an acrylic backplate to

[DOI: 10.1299/mej.16-00162]

remove the waviness of the surface. In addition, a smooth glass plate has been used as a reference surface. The specimens are then insonified with ultrasonic wave at normal incidence angle to the surface, as shown in Fig. 7. Here, a rectangular 0.4 MHz transducer having an element size of 15 mm x 20 mm has been employed and a square pulse has been used as the input signal. It is important to note here that the separation distance between the transducer and the specimens, as well as the reference surface, is required to be kept constant so that the accuracy of the measurement is independent from the separation distance. Thus, in this study, a constant distance of 30 mm has been used in all of the measurements. The signal fluctuations due to electrical and environmental noises in the measurements are reduced by taking an average of three hundred ultrasonic signals. The averaged signals from each specimen are then measured and used in the analysis.

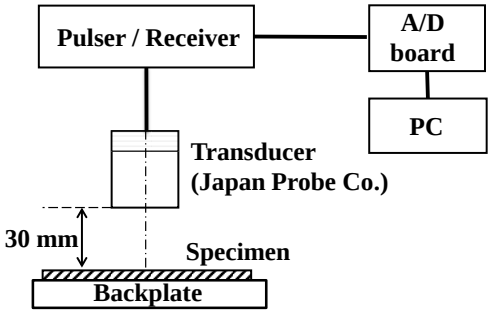

Fig. 7 Schematic of the experimental setup.

5.2 Experimental results and discussion

Figure 8 shows a typical reflected ultrasonic waveform and its corresponding frequency spectrum measured by the measurement system shown in Fig. 7. It is important to note here that the amplitudes at a specific frequency must be used in Eq. (20) to estimate the reflection coefficient of ultrasonic wave. In this study, the measured amplitude at frequency 0.35 MHz, which is the frequency of the peak amplitude of the reference surface (glass plate), is employed for the I estimation of each specimen. These amplitudes are then normalized by that of the reference surface and used for the characterization of non-Gaussian rough surfaces.

Moreover, we noted that the measurements in this study have been conducted in the near-field region even though theoretically, r is assumed to be in the far field region. For the transducer used in this study, the near field distance is approximately 115 mm, which makes the total propagation distance of the ultrasonic waves in a pulse-echo technique is 230 mm. At such distance, the signal-to-noise ratio (SNR) of measured ultrasonic signals becomes very low due to a very high attenuation in the air, resulting in decreasing measurement accuracy. Considering such trade-off relation between the distance r and SNR, the measurement in the near field region is inevitable in some cases and considered to be reasonable within a tolerable measurement error. Thus, r = 30 mm has been used in this work, which is an optimum distance providing sufficient intensity and SNR for the estimations of I. Nevertheless, it is noted that the ultrasonic measurements in the near field region should be avoided if possible in order to realize stable measurements.

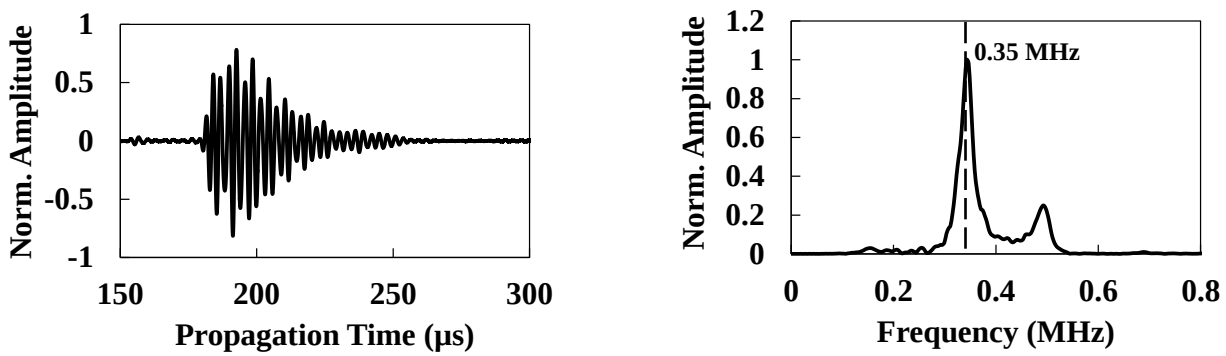

Fig. 8 Measured ultrasonic waveform (left) and the corresponding frequency spectrum (right).

[DOI: 10.1299/mej.16-00162]

Figure 9 shows the measured ultrasonic reflection coefficient I_{UT} (denote by black triangle) for all of the specimens. In general, it is observed that as Rq_{SP} increases, I_{UT} decreases. However, it is not always true especially for the specimens having similar Rq_{SP} but different Rsk_{SP}, where those with higher Rsk_{SP} values tend to have higher I_{UT} values, such as the specimen with Rq_{SP} = 50 μm and Rsk_{SP} = 0.34 and the one with Rq_{SP} = 54 μm and Rsk_{SP} = 0.92. Such differences in the measured I_{UT} for the specimens with similar Rq_{SP} but different Rsk_{SP} provide experimental evidences which support our finding from Fig. 6 where, for a constant value of Rq, an increase in the Rsk value will result in an increase in the reflection coefficient.

In addition, the experimentally measured I_{UT} are compared not only with the theoretical values of I_{MK} given by Eq. (20), but also with the values of I_{OK} given by Eq. (19). Such comparisons among I_{UT}, I_{OK} and I_{MK} are also shown in Fig. 9. It can be observed in Fig. 9 that the values of I_{MK} have a better agreement with I_{UT} compared to those of I_{OK}. This is because the effect of Rsk to the reflection coefficient has been taken into consideration in Eq. (19), where the existence of such Rsk indicates that the rough surfaces can be divided into two areas: a relatively small region consists of high peaks or deep valleys that scattered the incoherent ultrasonic waves and a relatively large region of the bearing surfaces with small height variations that reflected the ultrasonic waves coherently.

Moreover, to demonstrate further the validity of the derived theoretical relationship, the Rq of the specimens have been quantitatively estimated from the measured reflection coefficient I_{UT} by using the following equation

$$Rq_{UT-MK} = \sqrt{\ln\left(I_{MK}\right) \Big/ -2k^2 \left\{\frac{1.864 + 0.059\,|Rsk|}{1.864 + |Rsk|}\right\}^2}, \tag{21}$$

which has been derived from Eq. (20). For comparison purpose, Eq. (19) is also rearranged to ultrasonically estimate Rq of the specimens based on the original Kirchhoff theory using the same value of I_{UT}, and it is given by

$$Rq_{UT-OK} = \sqrt{\ln\left(I_{OK}\right) / -2k^2}. \tag{22}$$

Both ultrasonically estimated $Rq_{UT\text{-}MK}$ and $Rq_{UT\text{-}OK}$ are then compared with those measured by the stylus profiler, Rq_{SP}, and shown in Fig. 10. As a result, it can be observed that some of the $Rq_{UT\text{-}OK}$ values do not agree well with the corresponding Rq_{SP} values, especially for the specimens having large values of Rsk_{SP}. These results show that the straightforward implementation of the original Kirchhoff theory to the roughness characterization of the non-Gaussian rough surfaces by ultrasonic method could cause inaccurate estimations of the Rq value. On the other hand, a good agreement between the $Rq_{UT\text{-}MK}$ and Rq_{SP} with approximately 10% of errors is obtained. Such errors might be caused by the deviation of the height PDF of the bearing surfaces areas of the specimens from the Gaussian distribution or the difference in the actual Rku values of the specimens compared to the theoretical ones. Nevertheless, these experimental

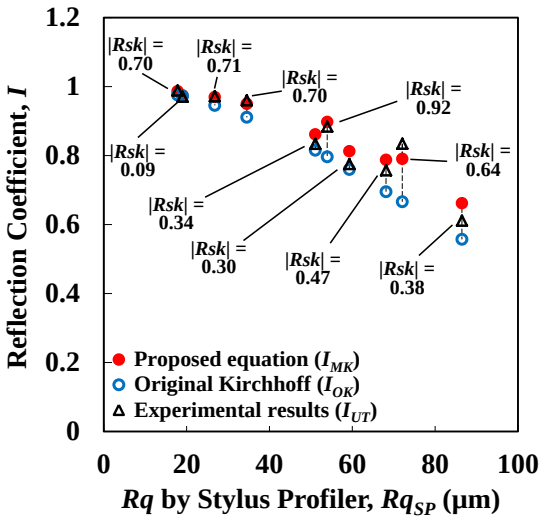

Fig. 9 Changes of the reflection coefficient with Rq.

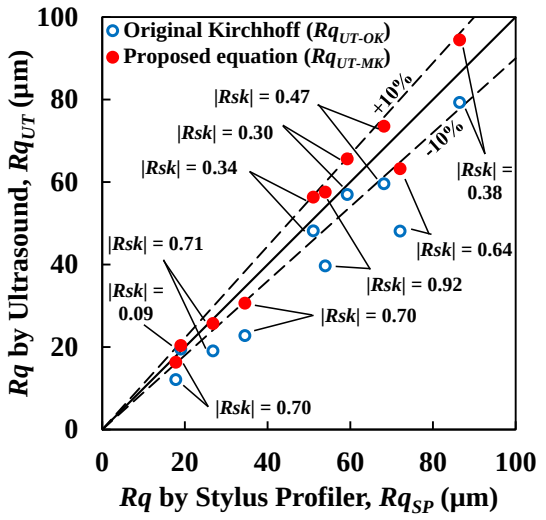

Fig. 10 Comparison between the profilometric and ultrasonic Rq estimated by the original Kirchhoff theory (OK) and the proposed equation (MK).

[DOI: 10.1299/mej.16-00162]

results provide evidences that confirm the validity of the derived theoretical relationship, and at the same time, demonstrate the potential of such relationship in the practical characterization of the non-Gaussian rough surfaces by ultrasonic method.

However, it is important to note here that in Eq. (21), the value of *Rsk* is needed to be known in order to estimate *Rq* from the reflection coefficient. Thus, the values of Rsk_{SP}, which are considered as the true skewness value of the specimens, have been used. Since the main objective of this study is to confirm the validity of the derived theoretical relationship, the uses of such Rsk_{SP} in estimating the values of $Rq_{UT\text{-}MK}$ is reasonable, such that any unnecessary errors caused by inaccurate *Rsk* values can be avoided. In practice, it is necessary to determine both *Rq* and *Rsk* values nondestructively by ultrasonic method in order to quantitatively characterize the non-Gaussian rough surfaces. However, to the best of the authors' knowledge, currently, there is no available ultrasonic method that is able to do so. In fact, this study is among the first to develop such method. Therefore, it is hoped that the findings from this study could be useful to develop an effective ultrasonic method that is able to quantitatively estimate not only the *Rq*, but also the *Rsk* of non-Gaussian surfaces.

6. Conclusion

To quantitatively characterize non-Gaussian rough surfaces of materials, a theoretical relationship among ultrasonic reflection coefficient at normal incidence, and two kinds of roughness parameters, *Rq* and *Rsk*, has been derived based on a Gaussian curve fitting to the non-Gaussian height distribution (the Johnson distribution) of a rough surface. Using the derived equation, the changes of the reflection coefficient with *Rq* for different *Rsk* values have been estimated numerically with artificially prepared non-Gaussian height distributions. It has been clearly found from the estimations that the reflection coefficient significantly depends on not only *Rq*, but also *Rsk* values. Then, the validity of the derived relationship has been verified experimentally where the *Rq* values estimated ultrasonically from the derived relationship are consistent with those measured using a stylus profiler. On the other hand, there exists large discrepancies between the *Rq* estimated ultrasonically using the original Kirchhoff equation and those measured using a stylus profiler. This reveals that the straightforward implementation of the original Kirchhoff equation to the *Rq* estimation of the non-Gaussian rough surfaces does not work properly. Based on the present study, the development of an effective method for determining either *Rq* or *Rsk* quantitatively from the measured ultrasonic reflection coefficient will be conducted as a future work. Moreover, the ultrasonic characterization of non-Gaussian rough surfaces in the far field region will also be considered in the future work.

Acknowledgement

This work was supported by the Grant-in-Aid for Scientific Research (B25289238) from the Japan Society for the Promotion of Science is greatly appreciated.

Appendix A

The derivation of Eq. (20) has been done by following the mathematical works by Ogilvy (Ogilvy, 1991). When a monochromatic plane wave is incidence to a perfectly reflecting one dimensional rough surface *S*, the general solution of the Kirchhoff approximation for the wave field scattered at an observation point *r* away from the surface in the far field region is given by

$$A^{sc}(x) = \frac{-\mathrm{i}ke^{\mathrm{i}kr}}{4\pi r} 2F(\theta_{inc}, \theta_{ref}) \int_S e^{\mathrm{i}k\phi(x)} dx \tag{A1}$$

where θ_{inc} is the incidence angle, θ_{ref} is the reflection angle, k is the wavenumber, $\phi(x)$ is a phase function and $F(\theta_{inc}, \theta_{ref})$ is an angular factor, which are given by

$$\phi(x) = Ax + Ch(x), \tag{A2}$$

[DOI: 10.1299/mej.16-00162]

$$F(\theta_{inc},\theta_{ref}) = \frac{(1+\cos\theta_{inc}\cos\theta_{ref} - \sin\theta_{inc}\sin\theta_{ref})}{\cos\theta_{inc}+\cos\theta_{ref}}, \tag{A3}$$

respectively. Here, A and C are given by

$$A = \sin\theta_{inc} - \sin\theta_{ref}, \tag{A4}$$

$$C = -(\cos\theta_{inc} + \cos\theta_{ref}), \tag{A5}$$

respectively. From Eq. (A1), the scattered wave is phase-modulated by the amount of $k\phi(x)$, where such amount then determines the amplitude of the scattered field $A^{sc}(x)$ from any height point $h(x)$ of the rough surface. Based on Eq. (A2), the phase difference $\Delta\varphi$ between two waves scattered from two separate height points, h_1 at position x_1 and h_2 at position x_2, on the surface is given by

$$\begin{aligned}\Delta\varphi &= k\phi(x_2) - k\phi(x_1),\\ &= k\left\{(h_2 - h_1)(\cos\theta_{inc}+\cos\theta_{ref}) + (x_2 - x_1)(\sin\theta_{inc} - \sin\theta_{ref})\right\},\\ &= k\left\{dh(\cos\theta_{inc}+\cos\theta_{ref}) + dx(\sin\theta_{inc} - \sin\theta_{ref})\right\}.\end{aligned} \tag{A6}$$

The interference between these waves depends on the magnitude of $\Delta\varphi$ compared with π. In the specular direction, when $\Delta\varphi \ll \pi$, these waves will be almost in-phase and will constructively interfere. In contrast, when $\Delta\varphi \approx \pi$, these waves will be out-of-phase and destructively interfere, leading to reduction of the coherent field energy. For a non-Gaussian rough surface, the high peaks or deep valleys generally have a large dh and gradient dh/dx. Thus, the reflected wave from such surface features will have a large $\Delta\varphi$ and will be reflected to the non-specular directions, which lead to no contribution to the coherent field energy in the specular direction. The coherent field then may be determined by the specularly reflected waves from the bearing surface area. The amplitude of the coherent field is depending on the average value of Eq. (A6) across the surface, which then leads to the averaging of $A^{sc}(x)$ across the surface. Given that the surface length is $-L < x < L$ and it height $h(x)$ is a random variable having a stationary Gaussian height PDF $p(h)'_G$ with standard deviation Rq' and mean $t = 0$, the average scattered field is given by

$$\left\langle A^{sc}\right\rangle = A_{coh} = \frac{-ike^{ikr}}{4\pi r} 2F\int_{-\infty}^{\infty}\int_{-L}^{L} e^{ik(Ax+Ch)} p(h)'_G\, dhdx. \tag{A7}$$

As $p(h)'_G$ is a stationary Gaussian distribution, which is independent of position, and given by

$$p(h)'_G = \frac{1}{Rq'\sqrt{2\pi}}\exp\left(-\frac{\{h\}^2}{2Rq'^2}\right), \tag{A8}$$

the coherent field then become

$$\begin{aligned}A_{coh} &= \frac{-ike^{ikr}}{4\pi r} 2F\int_{-L}^{L} e^{ikAx}dx\int_{-\infty}^{\infty} e^{ikCh} p(h)'_G\, dh,\\ &= -\frac{ike^{ikr}}{4\pi r} 2F\left(\frac{-2\sin(kAL)}{kA}\right)\int_{-\infty}^{\infty} e^{ikCh} p(h)'_G\, dh,\\ &= A_0\int_{-\infty}^{\infty} e^{ikCh} p(h)'_G\, dh,\\ &= A_0\exp\left(-\frac{1}{2}k^2 Rq'^2\left\{\cos\theta_{inc}+\cos\theta_{ref}\right\}^2\right).\end{aligned} \tag{A9}$$

Here, A_0 is the scattered field from a smooth surface. Eq. (A6) is the same as Eq. (14) while Eq. (A9) become Eq. (20) when $\theta_{inc} = \theta_{ref} = 0$. In short, the amplitude of the reflection coefficient given by Eq. (20) is depending on the average value of the phase differences given by Eq. (14) across the bearing surface, where such surface is having a Gaussian height PDF with standard deviation Rq'.

[DOI: 10.1299/mej.16-00162]

References

Asiltürk, İ. and Akkuş, H., Determining the effect of cutting parameters on surface roughness in hard turning using the Taguchi method, Measurement, Vol.44, No.9 (2011), pp.1697-1704.

Billy, M., Cohen-Ténoudji, F., Quentin, G., Lewis, K. and Adler, L., Ultrasonic evaluation of geometrical and surface parameters of rough defects in solids, Journal of Nondestructive Evaluation, Vol.1, No.4 (1980), pp.249-261.

Blessing, G. V., Ryan, H. M., Eitzen, D.G. and Slotwinski, J.A., Ultrasonic measurements of surface roughness, Applied Optics, Vol.32, No.19 (1993), pp.3433-3437.

Eriten, M., Polycarpou, A. A. and Bergman, L. A., Effects of surface roughness and lubrication on the early stages of fretting of mechanical lap joints, Wear, Vol.271, No.11-12 (2011), pp.2928-2939.

Forouzbakhsh, F., Gatabi, J. R. and Gatabi, I. R., A new measurement method for ultrasonic surface roughness measurements, Measurement, Vol.42, No.5 (2009), pp.702-705.

Gadelmawla, E. S., Koura, M. M., Maksoud, T. M. A., Elewa, I. M. and Soliman, H. H., Roughness parameters, Journal of Materials Processing Technology, Vol.123, No.1 (2002), pp.133-145.

Gunarathne, G. P. P. and Christidis, K., Measurements of surface texture using ultrasound, IEEE Transactions on Instrumentation and Measurement, Vol.50, No.5 (2001), pp.1144-1148.

Jeng, Y., Impact of plateaued surface on tribological performance, Tribology Transactions, Vol.39 (1996), pp.354-361.

Johnson, N. L., Systems of frequency curves generated by methods of translation, Biometrika, Vol.36, No.1 (1949), pp.149-176.

Kubiak, K. J., Liskiewicz, T. W. and Mathia, T. G., Surface morphology in engineering applications: Influence of roughness on sliding and wear in dry fretting, Tribology International, Vol.44, No.11 (2011), pp.1427–1432.

Miko, E. and Nowakowski, Ł., Analysis and verification of surface roughness constitution model after machining process, Procedia Engineering, Vol.39 (2012), pp.395-404.

Mitri, F. G., Kinnick, R. R., Greenleaf, J.F. and Fatemi, M., Continuous-wave ultrasound reflectometry for surface roughness imaging applications, Ultrasonics, Vol.49, No.1 (2009), pp.10-14.

Ogilvy, J. A., Computer simulation of acoustic wave scattering from rough surfaces, Journal of Physics D: Applied Physics, Vol.21, No.2 (1988), pp.260-277.

Ogilvy, J. A., Theory of Wave Scattering from Random Rough Surfaces (1991), pp.73-94, Institute of Physic Publishing, Berlin.

Ramesh, S., Srinivasa, K. and Subramanya, K. P., The use of ultrasound for the investigation of rough surface interface, International Journal of Scientific Engineering and Technology, Vol.2, No.5 (2013), pp.331-335.

Saniman, M. N. F. and Ihara, I., Application of air-coupled ultrasound to noncontact evaluation of paper surface roughness, Journal of Physics: Conference Series, Vol.520 (2014), p.012016.

Srivastava, D. K., Agarwal, A. K. and Kumar, J., Effect of liner surface properties on wear and friction in a non-firing engine simulator, Materials & Design, Vol.28, No.5 (2007), pp.1632-1640.

Sukmana, D. D. and Ihara, I., Quantitative evaluation of two kinds of surface roughness parameters using air-coupled ultrasound, Japanese Journal of Applied Physics, Vol.46, No.5B (2007), pp.4508-4513.

Suryono, Kusminarto and Suparta, G. B., Estimation of solid material surface roughness using time-of-flight ultrasound immerse transducer, Journal of Materials Science and Engineering, Vol.4, No.8 (2010), pp.35-39.

Taylor, J. B., Carrano, A. L. and Kandlikar, S. G., Characterization of the effect of surface roughness and texture on fluid flow—past, present, and future, International Journal of Thermal Sciences, Vol.45, No.10 (2006), pp.962-968.

Tuenter, H. J. H., An algorithm to determine the parameters of SU-curves in the Johnson system of probability distributions by moment matching, Journal of Statistical Computation and Simulation, Vol.70, No.4 (2001), pp.325-347.

Uehara, K. and Sakurai, M., Bonding strength of adhesives and surface roughness of joined parts, Journal of Materials Processing Technology, Vol.127, No.2 (2002), pp.178–181.

Wang, T., Wang, L., Zheng, D., Zhao, X. and Gu, L., Numerical simulation method of rough surfaces based on random switching system, Journal of Tribology, Vol.137, No.2 (2015), p.021403.

Wen, H., Design factors affecting the initial roughness of asphalt pavements, International Journal of Pavement Research and Technology, Vol.4, No.5 (2011), pp.268-273.

[DOI: 10.1299/mej.16-00162]

Whitehouse, D. J., Handbook of Surface and Nanometrology (2003), Institute of Physics Publishing, Bristol.

Yan, X., Wang, X. and Zhang, Y., Influence of roughness parameters skewness and kurtosis on fatigue life under mixed elastohydrodynamic lubrication point contacts, Journal of Tribology, Vol. 136, No.3 (2014), p.031503.

Yuan, C. Q., Peng, Z., Yan, X. P. and Zhou, X. C., Surface roughness evolutions in sliding wear process, Wear, Vol.265, No.3-4 (2008), pp. 341–348.

[DOI: 10.1299/mej.16-00162]